# Crystal Structures of Secondary Arenedicarboxamides. An Investigation of Arene−Hydrogen Bonding Relationships in the Solid State

**Frederick D. Lewis,* Jye-Shane Yang, and Charlotte L. Stern**

*Contribution from the Chemistry Department, Northwestern University, 2145 Sheridan Road, Evanston, Illinois 60208*

*Received August 26, 1996*[⊗]

**Abstract:** The crystal structures of a family of six secondary arenedicarboxamides have been determined. Four rodlike arenedicarboxamides pack in one-dimensional tapes in which the hydrogen-bonded scaffold holds adjacent arenes at a fixed separation of 5 Å. The dihedral angles between the planes of adjacent arenes range from 0° (face-to-face) to 68° (edge-to-face). Two naphthalenedicarboxamides pack in two-dimensional sheets. The 2,6-naphthalenedicarboxamide packs in a highly puckered single-layer sheet with no arene−arene close contacts. The 1,4-naphthalenedicarboxamide packs in an unusual bilayer sheet with partial face-to-face overlap of naphthalenes from adjacent sheets. Force field calculations indicate that electrostatic interactions are dominated by hydrogen bonding within a single tape or sheet and that the energetics of crystal packing in tapes or sheets are very similar. Thus, the nonbonded interactions between neighboring tapes or sheets play an important role in the determination of the packing motif. In the case of the tape structures, adjacent tapes have close-packed edge-to-face or herringbone arene−arene interactions, whereas the sheet structures display $\pi$-stacking and C═O···H−C hydrogen bonding.

## Introduction

Hydrogen bonding and aromatic−aromatic interactions play important roles in supramolecular chemistry, in both natural[1] and artificial systems.[2] Self-assembly of molecular components using these interactions has been widely investigated and provides one approach to the development of molecular devices.[3] Hydrogen bonding can result in the formation of one-dimensional chains or tapes, two-dimensional sheets, and three-dimensional structures.[4] Aromatic−aromatic interactions are complicated by the spatially anisotropic nature of the aromatic rings. At least four distinct crystal packing modes have been identified for polynuclear aromatic hydrocarbons. Small arenes such as benzene, naphthalene, and anthracene display herringbone structures, while larger arenes pack as sandwich herringbone, $\gamma$- or $\beta$-structures, according to the classification of Desiraju and Gavezzotti.[5] Polymorphism involving different packing modes has been observed for substituted arenes including 9-cyanoanthracene,[6] dichlorostilbene,[7] and binaphthyl.[8]

Leiserowitz and Tuval[9] classified the structures of secondary dicarboxamides as belonging to either of two motifs. Diamides which pack in one-dimensional tapes are translationally related, and each molecule is hydrogen-bonded to two adjacent molecules with a separation of 5 Å (motif A, Figure 1a). Diamides which pack in two-dimensional sheets are glide- or $2_1$-axis-related, and each molecule is hydrogen-bonded to four adjacent molecules (motif B, Figure 1b). A second sheet motif (motif C, Figure 1c) in which the two diamide carbonyl groups are pointed in the same direction rather than opposite directions has not thus far been observed. The choice between tape and sheet motifs is known to be sensitive to the size of the *N*-substituent, X, and the spacer R (Figure 1).[9,10] While diamides with bulky X groups prefer sheet structures due to the steric hindrance in the corresponding tapes, sheet structures can be adopted only if the cavity enclosed by the four N−H···O═C hydrogen bonds and the two R groups can be filled by the X groups (Figure 1). In the case of the secondary diamides of aromatic dicarboxylic acids, arene−arene interactions as well as hydrogen bonding might be expected to influence crystal packing. We report here the results of our investigation of the crystal structures of the *N*,*N*-dimethylarenedicarboxamides **1**−**6** (Chart 1). Examples are found of all three motifs in Figure 1. Both arene−arene and aromatic

[⊗] Abstract published in *Advance ACS Abstracts,* November 15, 1996.

(1) For related studies see: (a) Murakami, Y.; Aoyama, Y.; Kikuchi, J.; Nishida, K. *J. Am. Chem. Soc.* **1982**, *104*, 5189. (b) Burley, S. K.; Petsko, G. A. *J. Am. Chem. Soc.* **1986**, *108*, 7995. (c) Schweitzer, B. A.; Kool, E. T. *J. Am. Chem. Soc.* **1995,** *117*, 1863.

(2) For recent examples see: (a) Ferguson, S. B.; Sanford, E. M.; Seward, E. M.; Diederich, F. *J. Am. Chem. Soc.* **1991,** *113*, 5410. (b) Bisson, A. P.; Carver, F. J.; Hunter, C. A.; Waltho, J. P. *J. Am. Chem. Soc.* **1994,** *116*, 10292. (d) Shetty, A. S.; Zhang, J.; Moore, J. S. *J. Am. Chem. Soc.* **1996,** *118*, 1019. (e) Kennan, A. J.; Whitlock, H. W. *J. Am. Chem. Soc.* **1996**, *118*, 3027. (f) Qi, J.; Li, X.; Yang, X.; Seeman, N. C. *J. Am. Chem. Soc.* **1996**, *118*, 6121.

(3) (a) Lehn, J.-M. *Supramolecular Chemistry*, 1st ed.; VCH: New York, 1995. (b) Philp, D.; Stoddart, J. F. *Angew. Chem., Int. Ed. Engl.* **1996**, *35*, 1155.

(4) (a) MacDonald, J. C.; Whitesides, G. M. *Chem. Rev.* **1994**, *94*, 2383 and references cited therein. (b) Navarro, E.; Alemán, C.; Puiggalí, J. *J. Am. Chem. Soc.* **1995,** *117*, 7307. (c) Schwiebert, K. E.; Chin, D. N.; MacDonald, J. C.; Whitesides, G. M. *J. Am. Chem. Soc.* **1996**, *118*, 4018. (d) Aoyama, Y.; Endo, K.; Anzai, T.; Yamaguchi, Y.; Sawaki, T.; Kobayashi, K.; Kanehisa, N.; Hashimoto, H.; Kai, Y.; Masuda, H. *J. Am. Chem. Soc.* **1996**, *118*, 5562.

(5) (a) Gavezzotti, A. Desiraju, G. R. *Acta Crystallogr.* **1988**, *B44*, 427. (b) Desiraju, G. R.; Gavezzotti, A. *J. Chem. Soc., Chem. Commun.* **1989**, 621.

(6) Cohen, M. D.; Ludmer, Z.; Yakhot, V. *Phys. Status Solidi* **1975**, *67b*, 51.

(7) Cohen, R.; Ludmer, Z.; Yakhot, V. *Chem. Phys. Lett.* **1975**, *34*, 271.

(8) Kress, R. B.; Duesler, E. N.; Etter, M. C.; Paul, I. C.; Curtin, D. Y. *J. Am. Chem. Soc.* **1980**, *102*, 7709.

(9) Leiserowitz, L.; Tuval, M. *Acta Crystallogr.* **1978**, *B34*, 1230.

(10) (a) Harkema, S.; Gaymans, R. J. *Acta Crystallogr.* **1977**, *B33*, 3609. (b) Adams, W. W.; Fratini, A. V.; Wiff, D. R. *Acta Crystallogr.* **1978**, *B34*, 954. (c) Harkema, S.; Gaymans, R. J.; van Hummel, G. J.; Zylberlicht, D. *Acta Crystallogr.* **1979**, *B35*, 506 (d) Brisson, J.; Brisse, F. *Can. J. Chem.* **1985**, *63*, 3390. (e) Brisson, J.; Gagné, J. Brisse, F. *Can. J. Chem.* **1989**, *67*, 840. (f) Garcia-Tellado, F.; Geib, S. J.; Goswami, S.; Hamilton, A. D. *J. Am. Chem. Soc.* **1991,** *113*, 9265.

S0002-7863(96)02986-1 CCC: $12.00 

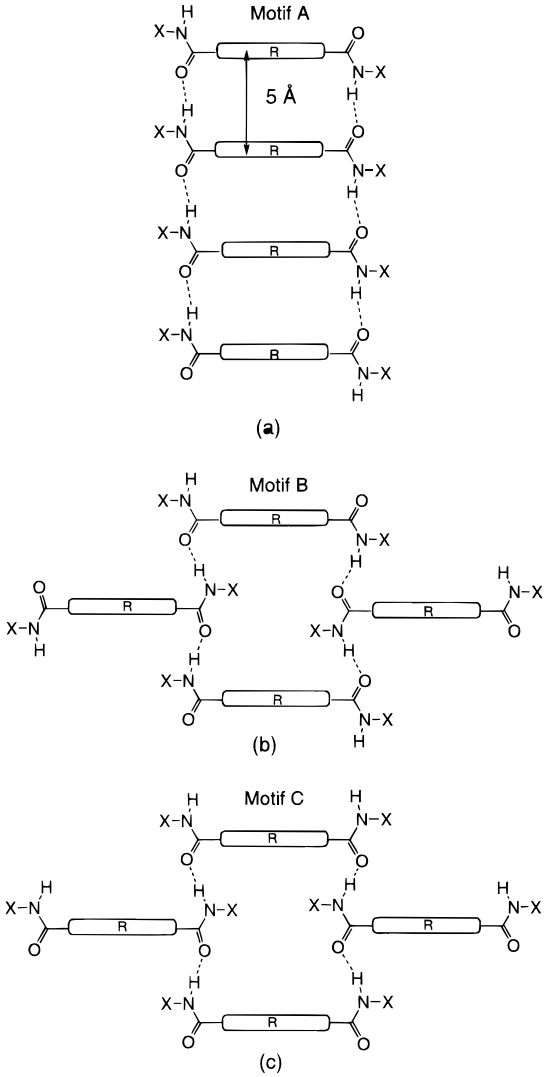


**Figure 1.** Schematic representations of the hydrogen-bonding motifs formed by secondary dicarboxamides X−NHOC−R−CONH−X: (a) a one-dimensional tape (motif A), (b) a two-dimensional sheet with opposite carbonyl orientations (motif B), and (c) a two-dimensional sheet with the same carbonyl orientations (motif C).

**Chart 1**

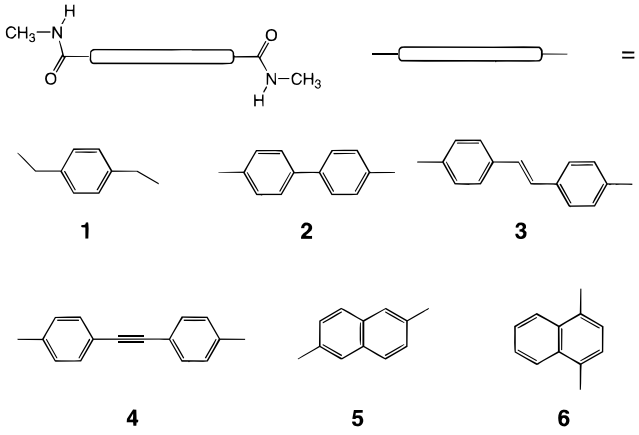


C−H···O═C interactions influence the choice of motif and the molecular geometry within the crystal.

## Experimental Section

**General Methods**. $^1$H NMR and $^{13}$C NMR (proton-decoupled) spectra were recorded in DMSO-$d_6$ solution using a Varian Gemini 300 spectrometer with TMS as internal standard. Infrared spectra were recorded on a Mattson FT-IR spectrometer. Elemental analysis were determined by Oneida Research Services Inc., Whitesboro, NY. Melting points were determined on a DuPont 910 differential scanning calorimeter with a DuPont model 200 thermal analyzer. The temperature was increased by 10 °C/min from 0 to 400 °C. The temperature was calibrated against zinc (mp = 419.5 °C) and tin (mp = 231.9 °C) metal.

Single crystals of **1**−**6** were obtained by slow evaporation of solvent from dilute solutions in mixed solvents (3:1 methanol−benzene for **1**, **2**, and **6** and 5:1 methanol−dimethyl sulfoxide for **3**−**5**). Data for all X-ray structures were recorded using an Enraf-Nonius CAD4 diffractometer with graphite-monochromated Mo Kα radiation ($\lambda$ = 0.710 69 Å) at −120 ± 1 °C. Numerical details pertaining to the collection of data, data processing, and refinement of the structures are given in Table 1. ORTEP drawings of the molecular structures and crystal-packing motifs and tables of positional and thermal parameters, bond lengths, and bond angles for **2**−**4** have been previously reported.[11] Corresponding data for **1**, **5**, and **6** are reported as Supporting Information.

All energy calculations used the Tripos 5.2 force field parameters[12] provided by the SYBYL[13] package for van der Waals and electrostatic interactions. The van der Waals terms were truncated at 8 Å from a central molecule, but include entire molecules located partially inside this distance. Charges were calculated using the Pullman method,[14] and a dielectric constant of 1.0 was employed. Crystal structures were used as the starting point for energy minimization, which was continued until the gradient in energy reached 0.05 kcal/mol or the number of iterations reached 1000. The interaction energies in a crystal and in a tape or a sheet were obtained by calculating the energy difference of the energy-minimized crystal, tape, or sheet with and without the central molecule.

**Syntheses**. Secondary dicarboxamides **1**−**6** were prepared from the corresponding dicarboxylic acids using standard procedures.[15] The dicarboxylic acid precursors of **1**−**3** (Aldrich) and **5** and **6** (TCI America) were used as received, and that of **4** was synthesized by the method of Lee and Marvel.[16] The dicarboxylic acids were converted to the corresponding diacid chlorides by reaction with thionyl chloride, and the diacid chlorides then reacted with methylamine gas (Fluka) or 40% aqueous solution (Aldrich) to give the corresponding dicarboxamides.

***N,N′*-Dimethyl-1,4′-phenylenediacetamide (1).** Mp = 214 °C. $^1$H NMR (DMSO-$d_6$): $\delta$ 7.94 (d, $J$ = 3.9 Hz, 2H), 7.15 (s, 4H), 3.33 (s, 4H), 2.56 (d, $J$ = 4.1 Hz, 6H). $^{13}$C NMR (DMSO-$d_6$): $\delta$ 170.5, 134.4, 128.8, 42.0, 25.6. IR (KBr): 3307, 1649, 1563, 1167 cm$^{-1}$. Anal. Calcd for $C_{12}H_{16}N_2O_2$: C, 65.43; N, 12.72; H, 7.32. Found: C, 65.88; N, 12.72; H, 7.35.

***N,N′*-Dimethyl-4,4′-biphenyldicarboxamide (2).** Mp = 324 °C. $^1$H NMR (DMSO-$d_6$): $\delta$ 8.54 (d, $J$ = 4.4 Hz, 2H), 7.95 (d, $J$ = 8.3 Hz, 4H), 7.83 (d, $J$ = 8.2 Hz, 4H), 2.81 (d, $J$ = 4.1 Hz, 6H). $^{13}$C NMR (DMSO-$d_6$): $\delta$ 166.1, 141.5, 133.7, 127.7, 126.7, 26.3. IR (KBr): 3287, 1642, 1543, 1411, 1318 cm$^{-1}$. Anal. Calcd for $C_{16}H_{16}N_2O_2$: C, 71.62; N, 10.44; H, 6.01. Found: C, 71.64; N, 10.40; H, 6.12.

***N,N′*-Dimethyl-4,4′-stilbenedicarboxamide (3).** Mp = 338 °C. $^1$H NMR (DMSO-$d_6$): $\delta$ 8.48 (d, $J$ = 4.4 Hz, 2H), 7.86 (d, $J$ = 8.3 Hz, 4H), 7.71 (d, $J$ = 8.0 Hz, 4H), 7.42 (s, 2H), 2.79 (d, $J$ = 4.3 Hz, 6H). $^{13}$C NMR (DMSO-$d_6$): $\delta$ 166.1, 139.4, 133.5, 129.2, 127.5, 126.5, 26.3. IR (KBr): 3308, 1631, 1543, 1459, 1317 cm$^{-1}$. Anal. Calcd for $C_{18}H_{18}N_2O_2$: C, 73.45; N, 9.52; H, 6.16. Found: C, 73.68; N, 9.43; H, 6.22.

***N,N′*-Dimethyl-4,4′-diphenylacetylenedicarboxamide (4).** Mp = 293 °C. $^1$H NMR (DMSO-$d_6$): $\delta$ 8.57 (d, $J$ = 4.7 Hz, 2H), 7.89 (d,

(11) Lewis, F. D.; Yang, J.-S.; Stern, C. L. *J. Am. Chem. Soc.* **1996**, *118*, 2772.
(12) Clark, M.; Cramer III, R. D.; Opdenbosch, N. V. *J. Comput. Chem.* **1989**, *10*, 982.
(13) A product of Tripos, Inc.
(14) The Pullman method, a combination of methods of Del Re and Hückel, can be found in the SYBYL program.
(15) (a) Burdett, K. A. *Synthesis* **1991**, 441. (b) Salunkhe, M.; Wu, T.; Letsinger, R. L. *J. Am. Chem. Soc.* **1992**, *114*, 8768. (c) Stella, L.; Raynier, B.; Surzur, J. M. *Tetrahedron Lett.* **1977**, 2721.
(16) Lee, B. H.; Marvel, C. S. *J. Polym. Sci., Chem. Ed.* **1982**, *20*, 393.

**Table 1.** Crystallographic Data

| | **1** | **2** | **3** | **4** | **5** | **6** |
|---|---|---|---|---|---|---|
| formula | $C_{12}H_{16}N_2O_2$ | $C_{16}H_{16}N_2O_2$ | $C_{18}H_{18}N_2O_2$ | $C_{18}H_{16}N_2O_2$ | $C_{14}H_{14}N_2O$ | $C_{14}H_{14}N_2O_2$ |
| formula weight | 220.27 | 268.31 | 294.35 | 292.34 | 242.28 | 242.28 |
| crystal system | monoclinic | monoclinic | monoclinic | triclinic | monoclinic | triclinic |
| size (mm) | 0.54 × 0.20 × 0.18 | 0.49 × 0.15 × 0.15 | 0.33 × 0.32 × 0.08 | 0.45 × 0.26 × 0.09 | 0.30 × 0.43 × 0.51 | 0.50 × 0.20 × 0.10 |
| color of crystal | colorless | colorless | colorless | colorless | colorless | colorless |
| *a* (Å) | 13.345(6) | 9.831(4) | 9.889(2) | 5.853(2) | 6.276(3) | 7.984(3) |
| *b* (Å) | 4.891(2) | 19.812(4) | 22.248(3) | 8.417(4) | 9.708(2) | 8.729(2) |
| *c* (Å) | 9.073(3) | 7.049(2) | 6.970(2) | 17.354(5) | 9.873(4) | 9.445(3) |
| *a* (deg) | 90 | 90 | 90 | 118.14(3) | 90 | 104.27(2) |
| *b* (deg) | 103.33(3) | 101.40(2) | 102.85(2) | 94.51(3) | 95.91(4) | 99.97(2) |
| $\gamma$ (deg) | 90 | 90 | 90 | 98.26(4) | 90 | 104.71(2) |
| space group | $P2_1/c$ | $P2_1/c$ | $P2_1/c$ | $P\bar{1}$ | $P2_1/c$ | $P\bar{1}$ |
| Z | 2 | 4 | 4 | 2 | 2 | 2 |
| density$_{calcd}$ (g/cm$^3$) | 1.269 | 1.324 | 1.308 | 1.320 | 1.345 | 1.347 |
| *m*(Mo Ka), cm$^{-1}$ | 0.87 | 0.88 | 0.86 | 0.87 | 0.92 | 0.92 |
| range of trans. factors (analytical abs correction) | 0.98−0.99 | 0.99−0.99 | 0.98−0.99 | 0.98−0.99 | 0.96−0.97 | 0.96−0.99 |
| 2*q* range | 2.0−53.9 | 2.0−55.9 | 2.0−45.9 | 2.0−49.9 | 2.0−45.9 | 2.0−53.9 |
| *F*(000) | 236.00 | 568.00 | 624.00 | 308.00 | 256.00 | 256.00 |
| no. obsd ($I > 3.00s(I)$) | 870 | 1441 | 1225 | 1736 | 741 | 2147 |
| no. variables | 106 | 230 | 208 | 264 | 111 | 220 |
| *R* (%) | 4.7 | 5.0 | 4.1 | 3.6 | 3.3 | 3.8 |
| $R_w$ (%) | 4.1 | 3.9 | 3.5 | 3.7 | 3.4 | 4.2 |
| goodness of fit | 2.47 | 1.82 | 1.64 | 2.02 | 3.62 | 3.76 |
| largest diff peak (e$^-$/Å$^3$) | 0.19 | 0.26 | 0.16 | 0.21 | 0.18 | 0.29 |

$J$ = 8.5 Hz, 4H), 7.67 (d, $J$ = 8.5 Hz, 4H), 2.79 (d, $J$ = 4.5 Hz, 6H). $^{13}$C NMR (DMSO-$d_6$): $\delta$ 165.7, 134.5, 131.4, 127.4, 124.4, 90.5, 26.3. IR (KBr): 3323, 2349, 1631, 1553 cm$^{-1}$. Anal. Calcd for $C_{18}H_{16}N_2O_2$: C, 73.95; N, 9.58; H, 5.52. Found: C, 73.72; N, 9.47; H, 5.71.

***N,N′*-Dimethyl-2,6-naphthalenedicarboxamide (5).** Mp = 318 °C. $^1$H NMR (DMSO-$d_6$): $\delta$ 8.66 (d, $J$ = 4.5 Hz, 2H), 8.44 (s, 2H), 8.06 (d, $J$ = 8.4 Hz, 2H), 7.95 (d, $J$ = 8.7 Hz, 2H), 2.83 (d, $J$ = 4.5 Hz, 6H). $^{13}$C NMR (DMSO-$d_6$): $\delta$ 166.4, 133.2 (2C), 128.9, 127.0, 124.7, 26.4. IR (KBr): 3273, 1639, 1553, 1318 cm$^{-1}$. Anal. Calcd for $C_{14}H_{14}N_2O_2$: C, 69.40; N, 11.56; H, 5.82. Found: C, 69.40; N, 11.55; H, 5.93.

***N,N′*-Dimethyl-1,4-naphthalenedicarboxamide (6).** Mp = 268 °C. $^1$H NMR (DMSO-$d_6$): $\delta$ 8.53 (d, $J$ = 4.7 Hz, 2H), 8.17−8.21 (m, 2H), 7.57 - 7.60 (m, 2H), 7.56 (s, 2H), 2.85 (d, $J$ = 4.6 Hz, 6H). $^{13}$C NMR (DMSO-$d_6$): $\delta$ 168.6, 136.4, 129.8, 126.8, 125.7, 123.9, 26.1. IR (KBr): 3325, 1639, 1523, 1397, 1302, 1156 cm$^{-1}$. Anal. Calcd for $C_{14}H_{14}N_2O_2$: C, 69.40; N, 11.56; H, 5.82. Found: C, 69.57; N, 11.55; H, 5.87.

## Results and Discussion

**Molecular Structure**. Crystals of the arenedicarboxamides **1**−**6** were grown by slow evaporation of solvent under ambient conditions. They crystallize in either monoclinic or triclinic space groups (Table 1). Three views of their crystal structures are shown in Figures 2−7. Crystals of **6** grown from three different mixed solvents were found to have the same unit cell parameters, indicating that the observed crystal structure is probably the most stable form in the solid state. Each molecule in the crystal has the same geometry, except in the case of **4** for which there are two crystallographically independent conformers which mainly differ in their arene−amide dihedral angles (*vide infra*). There are several interesting aspects of the molecular structures of **1**−**6**. All of the bond lengths and bond angles are normal except for the unusually short ethylene bond length in **3** (1.313(4) Å vs the standard 1.337(6) Å[17] ). By analogy to similar observations for other *trans*-stilbene derivatives, this is most likely an artifact caused by dynamic averaging originating from the torsional vibration of the C−Ph bond.[18] The large deviation from normal bond length suggests that the hydrogen-bonding scaffold allows rotational motion around the intramolecular amide−amide axis even at −120 °C.

**Table 2.** Dihedral Angles of Amide Groups and Phenyl−Carbonyl Planes

| | 1 | 2 | 3 | 4 | 5 | 6 |
|---|---|---|---|---|---|---|
| amide O−C−N−C (deg) | 1.6 | 2.7 | 3.3 | 0.7 | 2.0 | 0.5 |
| | | 4.5 | 4.1 | 2.5 | | 0.7 |
| phenyl−carbonyl (deg) | 76.5[a] | 22.6 | 25.5 | 10.5[b] | 24.8 | 50.9 |
| | | 44.7 | 37.7 | 49.2 | | 66.1 |

[a] A methylene group separates the phenyl and carbonyl planes in **1**. [b] Two distinct conformers exist in the crystal, and one has a larger angle than the other.

The biphenyl in **2**, *trans*-stilbene in **3**, and diphenylacetylene in **4** all adopt conformations similar to those observed in the vapor or solution phase.[19] Both biphenyl and *trans*-stilbene are nonplanar with phenyl−phenyl dihedral angles of 35.5° and 28.1°, respectively, whereas diphenylacetylene is planar. The parent arenes of **2**−**4** are all planar in the crystal.[20] The planarity of biphenyl and stilbene has been attributed to close-packing forces. Evidently, these forces do not determine the molecular conformation of **2** and **3** in the solid state.

Dihedral angles for the amide groups and the phenyl−carbonyl planes of **1**−**6** are reported in Table 2. The *N*-methyl amide groups are essentially planar, with O−C−N−C dihedral angles less than 5º, as observed for other *N*-methyl amides.[9] The arene−carbonyl dihedral angles display large deviations from planarity, as seen in other secondary areneamides.[21] Nonplanarity diminishes the resonance interaction between the arene and carbonyl $\pi$ systems, but is a prerequisite for the formation of N−H···O bonds of optimal length by translational symmetry. Each diamide molecule in **1** and **5** is centrosymmetric and thus has the same arene−carbonyl dihedral angles, whereas the asymmetric unit comprises the entire molecule in the cases of **2**, **3**, and **6**, giving rise to two nonequivalent arene−

(17) *International Tables for X-ray Crystallography*; Kynoch Press: Birmingham, 1968; Vol. III.

(18) Ogawa, K.; Sano, T.; Yoshimura, S.; Takeuchi, Y.; Toriumi, K. *J. Am. Chem. Soc.* **1992**, *114*, 1041.

(19) (a) Traetteberg, M.; Frantsen, E. B.; Mijlhoff, F. C.; Hoekstra, A. *J. Mol. Struct.* **1975**, *26*, 57. (b) Rubio, M.; Merchán, M.; Ortí, E.; Roos, B. O. *Chem. Phys. Lett.* **1995**, *234*, 373. (c) Saebø, S.; Almlöf, J.; Boggs, J. E.; Stark, J. G. *J. Mol. Struct.: THEOCHEM* **1989**, *200*, 361.

(20) (a) Hoekstra, A.; Meertens, P.; Vos, A. *Acta Crystallogr.* **1975**, *B31*, 2813. (b) Hargreaves, A.; Hasan Rizvi, S. *Acta Crystallogr.* **1962**, *15*, 365. (c) Mavridis, A.; Moustakali-Mavridis I. *Acta Crystallogr.* **1977**, *B33*, 3612.

(21) Toriumi, Y.; Kasuya, A.; Itai, A. *J. Org. Chem.* **1990**, *55*, 259.

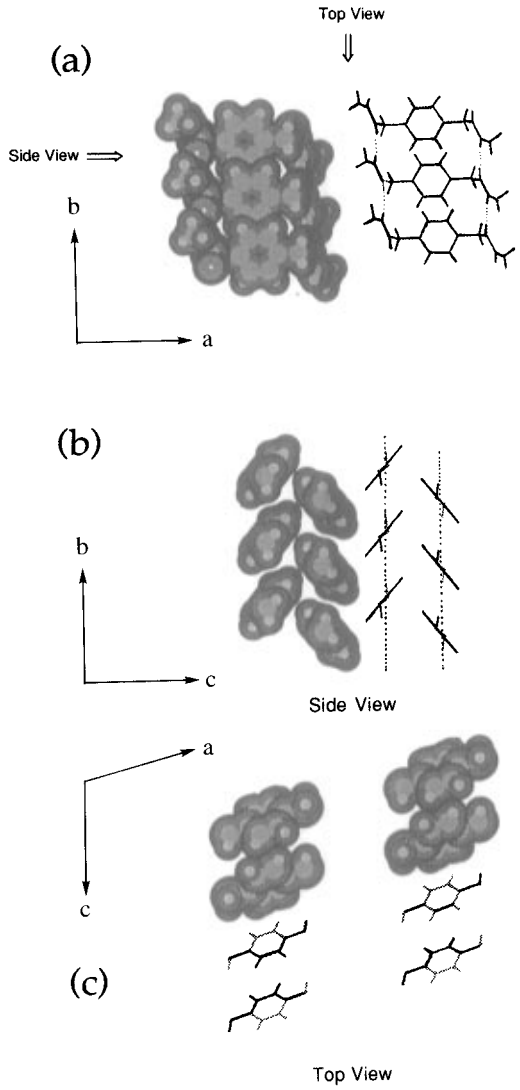


**Figure 2.** Three views of the packing arrangement for **1** using both of the space-filling and wire-frame models: (a) the offset, face-to-face xylene groups in the tapes, (b) side view of the tapes looking down the long axis (*a* direction) of the molecule (amide groups omitted for clarity) showing the herringbone packing of the xylene groups (hydrogen bonds expressed as the dotted lines), and (c) top view of the tapes looking down the hydrogen-bonding axis (*b* direction) of adjacent tapes.

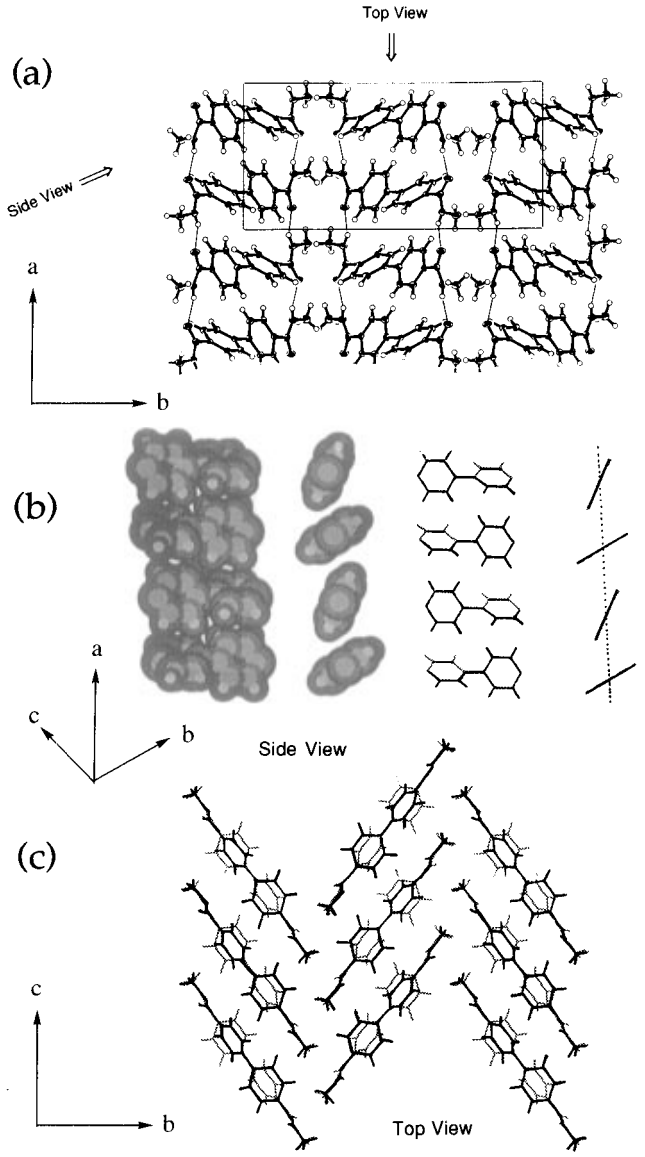


**Figure 3.** Three views of the packing arrangement for **2**: (a) an ORTEP drawing of the tapes, (b) side view of the tapes showing the edge-to-face phenyl−phenyl geometries using both the space-filling and wire-frame models (hydrogen-bonding axis expressed as a dotted line and amide groups omitted for clarity), and (c) top view of the tapes looking down the hydrogen-bonding axis (*a* direction) of adjacent tapes.

carbonyl dihedral angles. Two distinct centrosymmetic conformers exist in the crystal of **4**. Thus, the asymmetric unit contains half of each conformer in which one has arene−carbonyl dihedral angles of 10.5° and the other 49.2° (Figure 5a). The sums of the two nonequivalent dihedral angles in **2**−**4** are all in the range 60−67°. The largest dihedral angles are observed for **6**, presumably due to nonbonded repulsion between the carbonyl group and H-5 or H-8. It should be noted that a methylene group separates the phenyl ring and carbonyl in **1**, and thus the arene−carbonyl angles are not comparable to those in **2**−**6**.

**Hydrogen Bonding**. Dicarboxamides **1**−**4** adopt the translation-related packing motif A (Figure 1a), forming one-dimensional hydrogen-bonded tapes (Figures 2−5). The naphthalenedicarboxamides **5** and **6** adopt the glide-related motif B and the unusual pseudoglide (due to the pseudocrystallographic mirror symmetry of the molecule itself) related motif C (Figure 1), respectively, to form two-dimensional sheets (Figures 6 and 7). Structural parameters and solid state IR data for the hydrogen bonds are summarized in Table 3. Both of the hydrogen bonds in **1** and **5** are equivalent, whereas two slightly

**Table 3.** Structural and Solid State Infrared Data for Amide−Amide Hydrogen Bonds[a]

| | 1 | 2 | 3 | 4 | 5 | 6 |
|---|---|---|---|---|---|---|
| N(H)···O (Å) | 2.84 | 2.79 | 2.80 | 2.87 | 2.83 | 2.92 |
| | | 2.82 | 2.85 | 2.89 | | 2.93 |
| (N)H···O (Å) | 1.95 | 1.98 | 1.93 | 2.03 | 1.97 | 2.06 |
| | | 1.99 | 2.05 | 2.14 | | 2.22 |
| N−H···O (deg) | 179 | 155 | 159 | 139 | 164 | 137 |
| | | 159 | 162 | 160 | | 160 |
| H···O=C (deg) | 176 | 142 | 146 | 139 | 144 | 141 |
| | | 161 | 168 | 161 | | 159 |
| mean deviation from planarity (Å) | 0.0029 | 0.0006 | 0.0099 | 0.0523 | 0.0292 | 0.0170 |
| | | 0.0317 | 0.0364 | 0.1090 | | 0.0094 |
| $u_{C=O}$ (cm$^{-1}$) | 1639 | 1630 | 1631 | 1631 | 1639 | 1639 |
| $u_{N-H}$ (cm$^{-1}$) | 3298 | 3285 | 3308 | 3323 | 3273 | 3325 |

[a] Two values are shown in cases where the crystal possesses two nonequivalent hydrogen bonds.

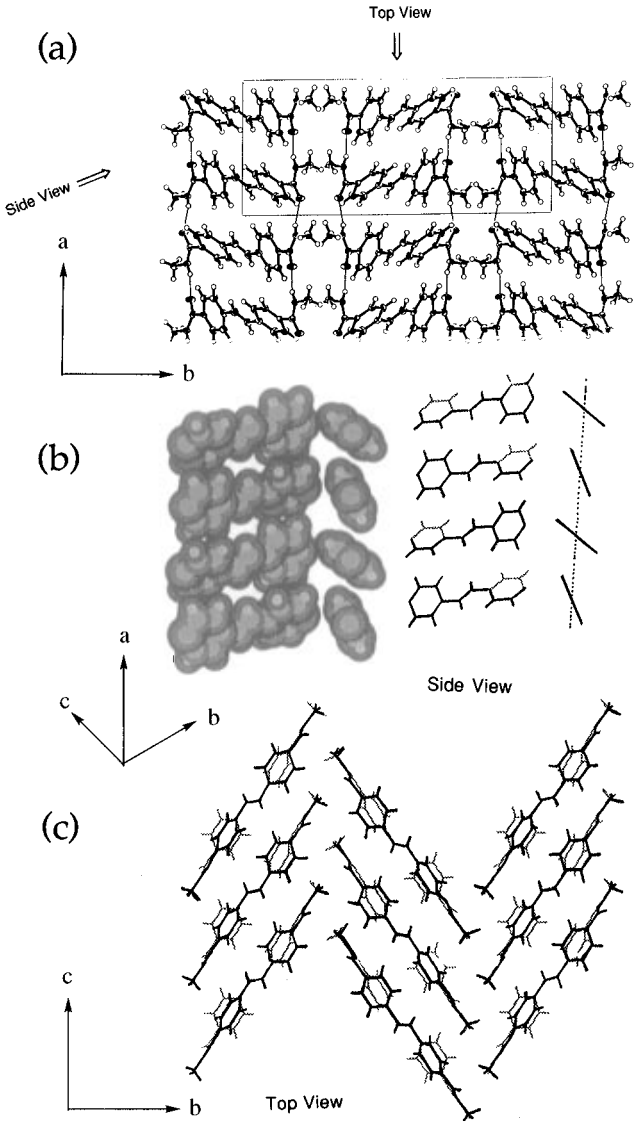


**Figure 4.** Three views of the packing arrangement for **3**: (a) an ORTEP drawing of the tapes, (b) side view of the tapes showing the edge-to-face phenyl−phenyl geometries using both the space-filling and wire-frame models (hydrogen-bonding axis expressed as a dotted line and amide groups omitted for clarity), and (c) top view of the tapes looking down the hydrogen-bonding axis (*a* direction) of adjacent tapes.

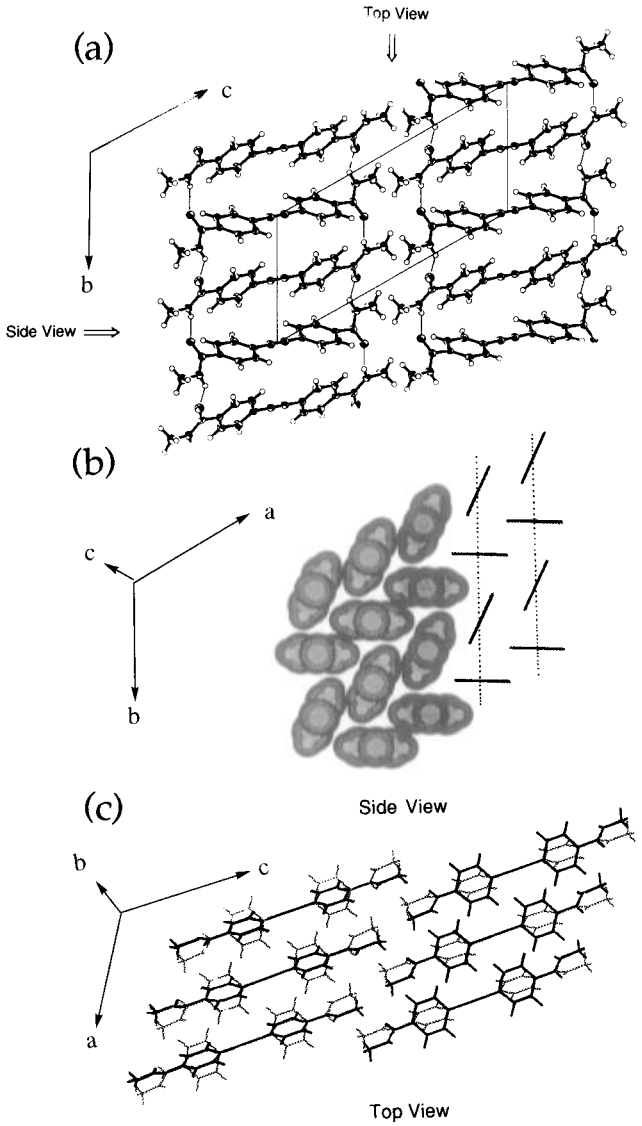


**Figure 5.** Three views of the packing arrangement for **4**: (a) an ORTEP drawing of the tapes, (b) side view of the tapes showing the herringbone packing of the diphenylacetylene groups using both the space-filling and wire-frame models (hydrogen-bonding axis expressed as dotted lines and amide groups omitted for clarity), and (c) top view of the tapes looking down the hydrogen-bonding axis of adjacent tapes.

different hydrogen bonds are observed in the other arenedicarboxamides.

The optimum geometry for amide−amide hydrogen bonding has linear and coplanar N−H···O bonds oriented in the direction of the oxygen $sp^2$ lone pairs.[9,22] The N(H)···O distances are all within the range of values observed by Leiserowitz and Tuval[9] for *N*-methyl mono- and dicarboxamides. The N−H···O angle for **1** is linear, but those for the other dicarboxamide are between 137° and 164°. The H···O═C angles are all larger than 120°. Mean deviations from planarity are small for all of the hydrogen bonds. Hydrogen bonding is known to decrease both the C═O and N−H IR stretching frequencies. While there are variations in these frequencies for **1**−**6** (Table 3), no consistent pattern emerges which might be indicative of differences in the relative hydrogen bond strengths. The arenedicarboxamides are highly insoluble in less polar solvents than dimethyl sulfoxide or alcohols, and thus it was not possible to obtain solution IR data for comparison with solid state IR and structural data.

(22) Taylor, R.; Kennard, O. *Acc. Chem. Res.* **1984**, *17*, 320.

The intermolecular N−$CH_3$···$CH_3$−N contacts in the idealized planar sheet motifs B and C shown in Figure 1 must be accomodated by distortion of the sheet structure if the group R is not sufficiently long. This is accomplished by puckering of the sheet in **5** and by distortion of the hydrogen-bonded network in **6**, which results in nonlinear N−H···O hydrogen bonding. Linear N−H···O bonding requires that the pseudoglide plane pass through the carbonyl C atoms, as the case in Figure 1c. For such a system, given 3.5 Å as the intermolecular $CH_3$···$CH_3$ distance, the separation between neighboring pseudoglide planes would be ca. 7.5 Å ($2 \times (1.45 + 1.25 \cos 60°) + 3.5$ Å). However, the intramolecular distance between the two carbonyl C atoms is only ca. 5.8 Å ($2 \times 1.5 + 2.8$ Å), which is obviouly not long enough to accommodate the N−$CH_3$···$CH_3$−N groups. As a result, the pseudoglide plane passes through the N and O atoms (Figure 7a), leading to nonlinear N−H···O bonds.

**Arene−Arene and Arene−Carbonyl Interactions**. The neighboring phenyl rings in a hydrogen-bonded tape of **1** adopt an offset, parallel geometry (Figure 2b). The plane-to-plane distance is 3.11 Å; however, there are no short contacts (<3.6

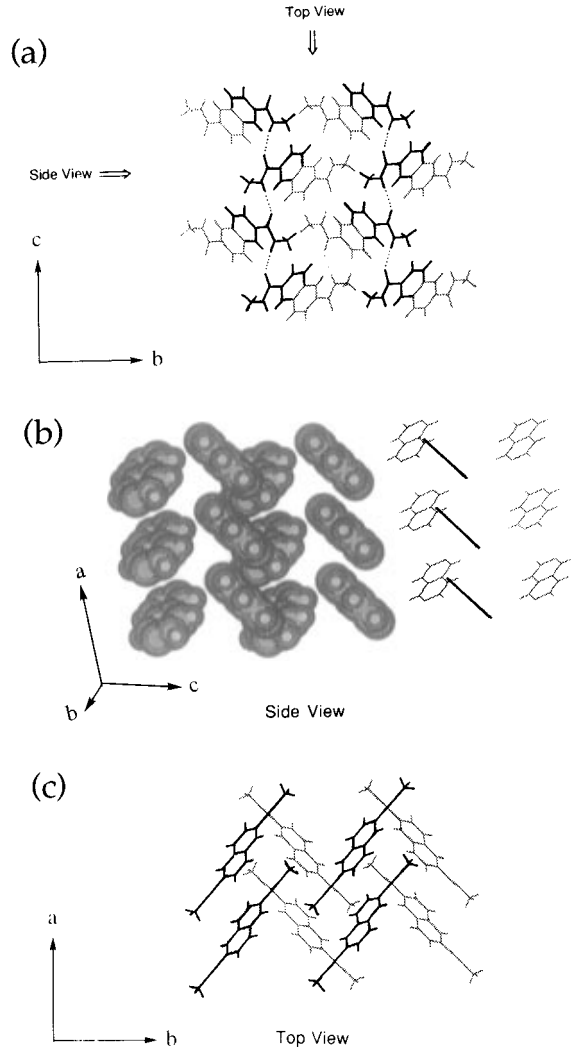


**Figure 6.** Three views of the packing arrangement for **5**: (a) a puckered sheet, (b) side view of the sheets showing the offset, face-to-face naphthalene−naphthalene geometries of adjacent sheets (amide groups omitted for clarity) using both the space-filling and wire-frame models, and (c) top view of the sheets looking down the hydrogen-bonding axis (*c* direction) of adjacent sheets.

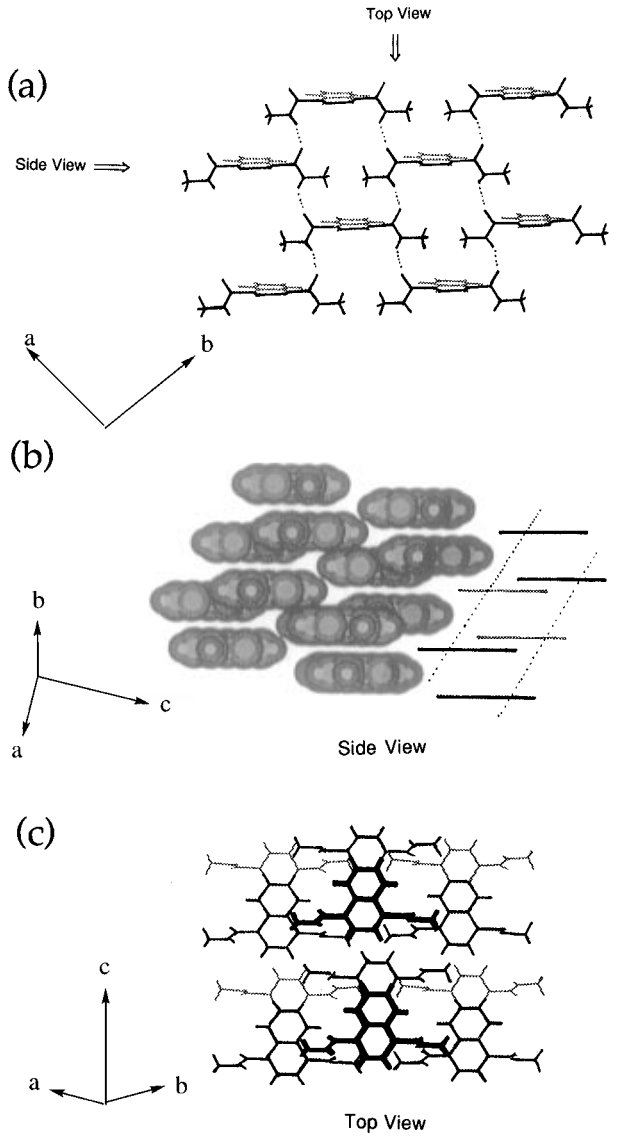


**Figure 7.** Three views of the packing arrangement for **6**: (a) a sheet, (b) side view of the sheets showing the pairwise, face-to-face naphthalene−naphthalene geometries and the bilayer structure of adjacent layers (hydrogen-bonding axis expressed as dotted lines amide groups omitted for clarity) using both the space-filling and wire-frame models, and (c) top view of the sheets looking down the hydrogen-bonding axis of adjacent sheets.

Å) between the carbon atoms of neighboring rings. In contrast, the neighboring phenyl rings in the hydrogen-bonded tapes of **2**−**4** adopt edge-to-face geometries (Figures 3b−5b), which are schematically depicted in Figure 8a (for **2** and **3**) and Figure 8b (for **4**). The averaged centroid−centroid distances between adjacent phenyl rings are in the order **3** (4.95 Å) ≈ **2** (4.92 Å) > **4** (4.77 Å), and phenyl−phenyl dihedral angles are in the order **4** (67.9°) > **2** (35.5°) > **3** (28.1°). Neighboring arene molecules in adjacent tapes of **1**−**3** also adopt edge-to-face geometries (Figures 2c−4c). The centroid−centroid distances between phenyl rings in adjacent tapes are 5.15, 4.48, and 4.40 Å, respectively, and the dihedral angles are 79.1°, 35.5°, and 28.1°. As a consequence of different symmetry relationships between the tapes, arenes in adjacent tapes of **4** are offset, parallel (Figure 5b,c) and have only one C···C contact shorter than 3.6 Å (Table 4). It is interesting to note that, in spite of their different arene−arene geometries within a tape, the herringbone-like three-dimensional phenyl−phenyl alignments in **1** and **4** are very similar (Figures 2b and 5b).

The crystal structures of **2**−**4** could readily accommodate offset, face-to-face phenyl−phenyl geometries as shown schematically in Figure 8c (for **2** and **3**) and Figure 8d (for **4**). Both the herringbone packing of arenes in **1** and **4** and the edge-to-face phenyl−phenyl alignments in **2** and **3** are consistent with the preference for edge-to-face vs face-to-face phenyl−phenyl geometry of benzene dimers in the gas and liquid phases and the herringbone structures in the crystal.[23−25] A phenyl−phenyl dihedral angle of 60° has been found to be the most common in the distribution of phenylalanine−phenylalanine dihedral angles observed for globular proteins.[26] The intertape dihedral angle in **1** and intratape angle in **4** are similar to that for phenylalanine−phenylalanine or the perpendicular benzene

(23) Jorgensen, W. L.; Severance, D. L. *J. Am. Chem. Soc.* **1990**, *112*, 4768.

(24) (a) Linse, P. *J. Am. Chem. Soc.* **1993**, *115*, 8793. (b) Linse, P. *J. Am. Chem. Soc.* **1992**, *114*, 4366. (c) Pettersson, I.; Liljefors, T. *J. Comput. Chem.* **1987**, *8*, 1139.

(25) (a) Janda, K. C.; Hemminger, J. C.; Winn, J. S.; Novick, S. E.; Harris, S. J.; Klemperer, W. *J. Chem. Phys.* **1975**, *63*, 1419. (b) Steed, J. M.; Dixon, T. A.; Klemperer, W. *J. Chem. Phys.* **1979**, *70*, 4940. (c) Law, K. S.; Schauter, M.; Bernstein, E. R. *J. Chem. Phys.* **1984**, *81*, 4871. (d) Börnsen, K. O.; Selzle, H. L.; Schlag, E. W. *J. Chem. Phys.* **1986**, *85*, 1726.(e) Laatikainen, R.; Ratilainen, J.; Sebastian, R.; Santa, H. *J. Am. Chem. Soc.* **1995**, *117*, 11006.

(26) Singh, J.; Thornton, J. M. *FEBS Lett.* **1985**, *191*, 1.

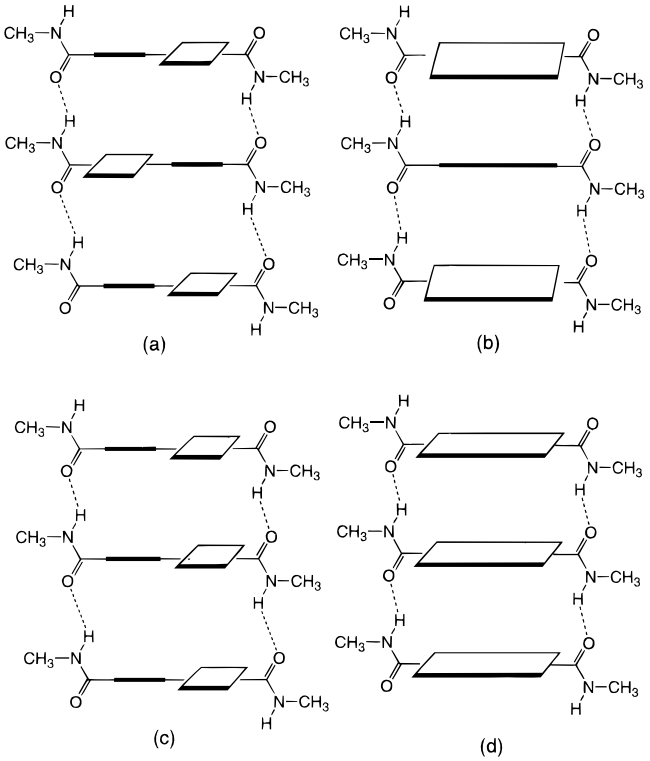


**Figure 8.** Schematic representations of the edge-to-face (a) phenyl−phenyl geometries in a tape for **2** and **3** and (b) diphenylacetylene−diphenylacetylene geometries for **4**, and the hypothetical offset, face-to-face arene−arene geometries for (c) **2** and **3** and for (d) **4**.

dimer. The smaller dihedral angles observed for **2** and **3** are determined by the optimum intramolecular phenyl−phenyl dihedral angles of the biphenyl and stilbene groups. For example, in the case of biphenyl **2**, an "optimized" edge-to-face geometry could be obtained for biphenyl intramolecular dihedral angles of either 0° (Figure 8b) or 90° (Figure 8a). The estimated energy required for converting biphenyl to either its planar or perpendicular conformation is ∼2 kcal/mol,[27] which may be higher than the energy gain which would result from an increase in the edge-to-face interaction.

Intermolecular C···C close contacts (<3.6 Å) for **1**−**6** are summarized in Table 4. There are no close arene−arene contacts between adjacent naphthalenes within the two-dimensional sheets of **5** or **6** (Figures 6a and 7a), as might be expected on the basis of the hydrogen-bonding scaffold (Figure 1b,c). The planes of the closest naphthalene in adjacent sheets of **5** and **6** are parallel (Figures 6c and 7c). In the case of **5**, the naphthalenes are offset with a plane-to-plane separation of 3.57 Å and there are no short C···C contacts (<3.6 Å, Figure 6b). In contrast naphthalenes in adjacent sheets of **6** have significant overlap (Figure 7b) and have a 3.48 Å plane-to-plane separation. These arene−arene interactions may contribute to the stabilization of the single-layer structure in **5** and the bilayer structure in **6**. Russell et al.[28] have observed that guanidinium 1-naphthalenesulfonate and 2-naphthalenesulfonate adopt single-layer and bilayer structures, respectively. Naphthalenes from adjacent layers adopt a face-to-face geometry in the former salt and a herringbone edge-to-face geometry in the latter.

In addition to arene−arene interactions, the arenedicarboxamides display some short C═O···H−C contacts both within a single tape or sheet and between adjacent tapes or sheets. The only short intratape contact involving an aromatic hydrogen is that observed in **4**. Particularly notable are the two very short contacts between the aromatic H-2 and H-3 and the two carbonyl oxygens of a dicarboxamide in the adjacent layer of **6** (Table 4). The lengths and angles for these contacts (Table 4) are consistent with Desiraju's criteria for strong C−H···O hydrogen bonding.[29] Both C−H···O hydrogen bonds are possible only when both carbonyl oxygens point in the same direction, as is the case for motif C, but not for motif B (Figure 1). However, face-to-face interactions between naphthalenes in adjacent tapes would be possible in motif B, as shown schematically in Figure 9, as well as motif C. Thus, it is possible that C−H···O hydrogen bonding rather than naphthalene−naphthalene interactions (Figure 7b) is responsible for the observation of the unusual motif-C bilayer structure of **6**. As a consequence of the motif-C packing of **6**, the nonbonded contact between the two adjacent methyl groups (X in Figure 1c) in the same layer is 0.12 Å shorter than the sum of the van der Waals radii (Table 4).

**Tapes vs Sheets (Force Field Calculations).** As mentioned previously, the formation of tape vs sheet structures by secondary dicarboxamides can be influenced by the *N*-substituent X as well as the nature of the linker R (Figure 1). The use of the small *N*-methyl substituent in this investigation permits us to focus on the role of arene−arene interactions in crystal packing. The observation of tape motifs for **1**−**4** with arene−arene geometries ranging from offset, face-to-face to edge-to-face and two different sheet motifs for **5** and **6** indicates that the crystal structures of the arenedicarboxamides are highly dependent upon arene structure. One possible explanation for the occurrence of sheet motifs for **5** and **6** is that the arene is effectively "wider" than the rodlike arenes of **1**−**4** (Figure 10). While this might prevent packing in an edge-to-face tape (Figure 8b), it should not interfere with packing in a face-to-face tape (Figure 8d). In fact a tape structure similar to **1** with face-to-face naphthalenes has been reported for a secondary diamide derivative of 2,6-naphthalenedicarboxylic acid with different *N*-substituents.[30] In addition, it was recently reported that the *N*,*N*′-dimethyl amide of *p*-phenylenediacrylic acid, which is a rodlike arene, packs in sheets (Figure 1b).[31] Evidently, the choice of crystal-packing motifs is dependent upon the interactions between adjacent tapes or sheets as well as the interactions between molecules within a single tape or sheet.

In order to compare the nonbonded interactions of arenedicarboxamides within a tape or a sheet with those between tapes or sheets, the Tripos 5.2 force field[12] in the SYBYL[13] package has been employed to obtain the electrostatic and van der Waals potential energies of **1**−**6**. The charges used for electrostatic energy calculations were calculated using the Pullman method,[14] and a dielectric constant of 1.0 was assumed. The van der Waals interactions were truncated at 8 Å. The single-crystal data served as the starting point for the geometry, and the energy of the crystal was minimized until the gradient in energy reached 0.05 kcal/mol or the number of iterations reached 1000. Since hydrogen bonding is an electrostatic phenomenon, the hydrogen-bonding energy is included in the electrostatic energy. The results of calculations for **1**−**6** are reported in Figure 11a. The van der Waals energies largely determine the relative lattice

(27) Takei, Y.; Yamaguchi, T.; Osamura, Y.; Fuke, K.; Kaya, K. *J. Phys. Chem.* **1988**, *92*, 577.
(28) Russell, V. A.; Etter, M. C.; Ward, M. D. *J. Am. Chem. Soc.* **1994**, *116*, 1941.
(29) (a) Taylor, R.; Kennard, O. *J. Am. Chem. Soc.* **1982,** *104*, 5063. (b) Desiraju, G. R. *Acc. Chem. Res.* **1991**, *24*, 290. (c) Desiraju, G. R. *Crystal Engineering-The Design of Organic Solid;* Elsevier: New York, 1989; pp 142−173. (d) Steiner, T.; Saenger, W. *J. Am. Chem. Soc.* **1993,** *115*, 4540. (e) Shimoni, L.; Carrell, H. L.; Glusker, J. P.; Coombs, M. M. *J. Am. Chem. Soc.* **1994,** *116*, 8162. (f) Desiraju, G. R. *Acc. Chem. Res.* **1996**, *29*, 441.
(30) Weinstein, S.; Leiserowitz, L.; Gil-Av, E. *J. Am. Chem. Soc.* **1980,** *102*, 2768.
(31) Feeder, N.; Nakanishi, F. *Mol. Cryst. Liq. Cryst. Sci. Technol., Sect. A* **1996**, *277*, 691.

**Table 4.** Intermolecular C···C (<3.6 Å) and O···H-C (<2.6 Å) Close Contact Distances between the Asymmetric Molecule[a] and Its Neighbors in the Same or Adjacent Hydrogen-Bonded Tapes or Sheets

| | within tapes or sheets | | | adjacent tapes or sheets | | |
|---|---|---|---|---|---|---|
| compound | distance (Å) | ± sum of VDW | atom *i*···atom *j* | distance (Å) | ± sum of VDW | atom *i*···atin *j* |
| **1**[b] | none | | | 3.35 | −0.05 | C(1)···C(1) |
| | | | | 3.52 | 0.12 | C(7)···C(7)[c] |
| | | | | 3.43 | 0.03 | C(7)···C(8)[c] |
| **2** | 3.56 | 0.16 | C(7)···C(14)[c] | 3.46 | 0.06 | C(1)···C(2) |
| | 3.53 | 0.13 | C(8)···C(13)[c] | 3.50 | 0.10 | C(4)···C(12)c |
| | | | | 3.55 | 0.15 | C(4)···C(13)[c] |
| | | | | 3.46 | 0.06 | C(5)···C(12)[c] |
| | | | | 3.41 | 0.01 | C(5)···C(15) |
| | | | | 3.56 | 0.16 | C(15)···C(16) |
| **3** | 3.56 | 0.16 | C(4)···C(13)[c] | 3.46 | 0.06 | C(1)···C(2) |
| | 3.48 | 0.08 | C(5)···C(13)[c] | 3.53 | 0.13 | C(4)···C(11)[c] |
| | 3.43 | 0.03 | C(7)···C(16)[c] | 3.53 | 0.13 | C(4)···C(16)[c] |
| | 3.45 | 0.05 | C(8)···C(15)[c] | 3.46 | 0.06 | C(5)···C(15)[c] |
| | 3.49 | 0.09 | C(8)···C(16)[c] | 3.48 | 0.08 | C(5)···C(16)[c] |
| | | | | 3.58 | 0.18 | C(10)···C(17) |
| **4** | 2.44 | −0.18 | O(2)···H(5)[d] | 3.48, 3.54 | 0.08, 0.14 | C(1)···C(11) |
| | | | | 3.59 | 0.19 | C(2)···C(12) |
| | | | | 3.59 | 0.19 | C(17)···C(17)[c] |
| **5** | none | | | none | | |
| **6** | 3.56 | 0.16 | C(6)···C(12) | 2.45 | −0.17 | O(1)···H(2)[e] |
| | 3.53 | 0.13 | C(7)···C(12) | 2.44 | −0.18 | O(2)···H(3)[f] |
| | 3.28 | −0.12 | C(12)···C(14) | 3.58 | 0.18 | C(1)···C(5)[c] |
| | | | | 3.49 | 0.09 | C(2)···C(6)[c] |
| | | | | 3.55 | 0.15 | C(4)···C(8)[c] |
| | | | | 3.54 | 0.14 | C(9)···C(9)[c] |

[a] Asymmetric molecules:

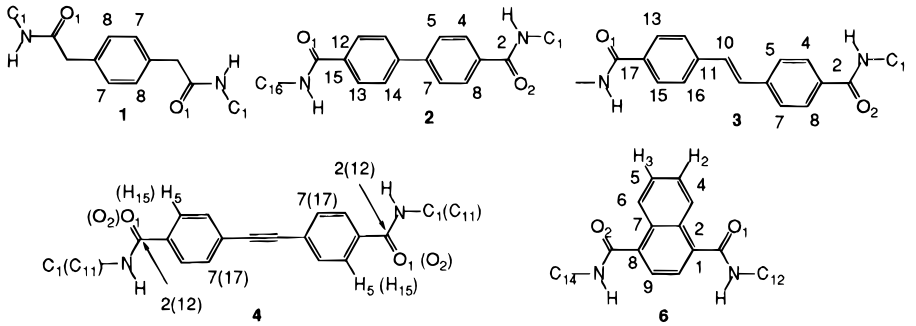

[b] The number of close contacts should be doubled for each molecule due to the symmetry of the inversion center. [c] Arene−arene carbons. [d] C−H···O = 151° and H···O=C = 109°. [e] C−H···O = 147° and H···O=C = 133°. [f] C−H···O = 167° and H···O=C = 119°.

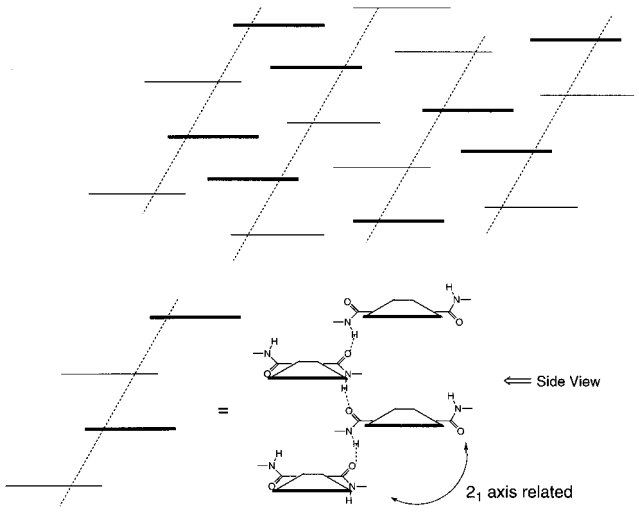


**Figure 9.** Schematic representations of the hypothetical single-layer and motif-B packings for **6** showing the pairwise, face-to-face naphthalene−naphthalene overlaps.

energies and appear to reflect the relative size of arenes (**3** ≈ **4** > **2** > **5** = **6** > **1**) rather than the presence or absence of arene−arene interactions. The smaller electrostatic energy for **6** vs **5** may explain the absence of prior examples of packing motif C (Figure 1). The electrostatic energy of **5** is larger than that for **1** and comparable to those of **2**−**4**, and thus the preference for packing in tape vs sheet structures is not determined by the total electrostatic energy.

The contribution of electrostatic and van der Waals energies within a tape or sheet to the total lattice energy of the crystal is reported in Figure 11b. Greater than 90% of the total electrostatic energy is contributed by the tapes or sheets, except in the case of **1**. This result is hardly surprising since amide−amide hydrogen bonding occurs only within individual tapes or sheets and dominates the electrostatic energy. The contribution of the tapes or sheets to the total van der Waals energy is <35%, and that to the total lattice energy is ∼50%. These results imply that interactions between tapes or sheets are as important as those within tapes or sheets. Similar findings have been used to interpret the anomalous packing of adipamide by Hagler and Leiserowitz.[32] Thus, in cases where both motifs are possible, favorable nonbonded interactions between tapes or sheets play an important role in the choice between tape and sheet structures. The edge-to-face arene−arene interactions and herringbone packings between adjacent tapes of **1**−**4** (Figures 2−4) may favor the tape vs sheet structure. It appears likely

(32) Hagler, A. T.; Leiserowitz, L. *J. Am. Chem. Soc.* **1978,** *100,* 5879.

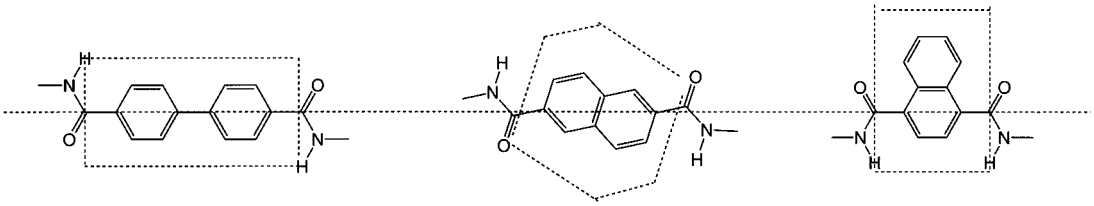

**Figure 10.** A comparision of the shape of the arenes biphenyl and naphthalene around the amide−amide axis.

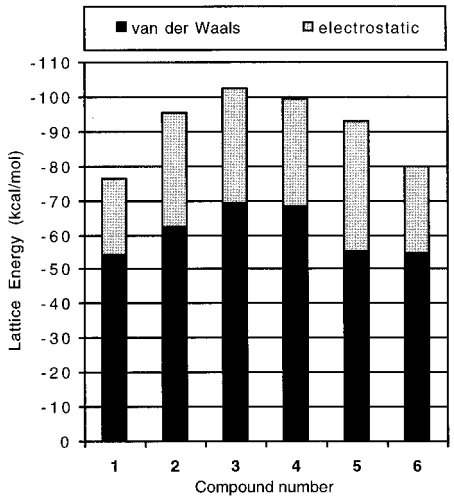


(a)

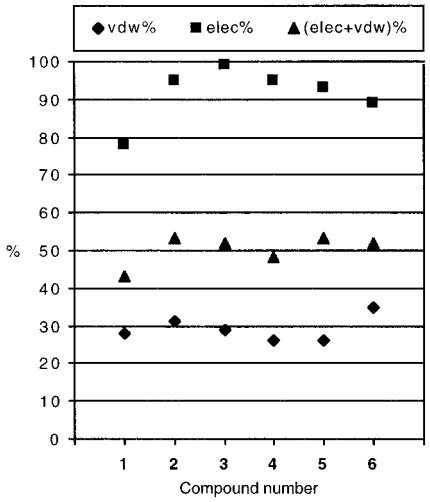


(b)

**Figure 11.** (a) Calculated lattic energy, including the electrostatic and van der Waals components and (b) the calculated percentage of contribution of electrostatic (elec%), van der Waals (vdw%), and total ((elec+vdw)%) energies within a tape or a sheet to the corresponding energies in a crystal for arenedicarboxamides **1**−**6**.

that tape structures of the wider naphthalenes in **5** and **6** would not possess favorable intertape interactions and would be loosely packed (Figure 10). Both face-to-face $\pi$-stacking and C−H···O═C hydrogen bonding between the adjacent sheets may contribute to the stability of the unusual bilayer structure for **6**. Whereas **5** does not display C−H···O═C hydrogen bonding, it has the same calculated density of 1.35 g/cm$^3$ as **6**, indicating close packing in both compounds. Such close packing might not be attained if **5** adopted a tape structure due to its wider arene shape. Likewise, the sheet structure observed in *N*,*N*-dimethyl amide of *p*-phenylenediacrylic acid,[31] a rodlike molecule, can be understood because its small vinyl−amide dihedral angles permit it to pack in a planar sheet motif (Figure 1b) with face-to-face $\pi$-stacking between sheets.

**Concluding Remarks**. The three hydrogen-bonding motifs available to single crystals of secondary arenedicarboxamides permit the investigation of arene−arene interactions both within a single tape or sheet and between adjacent tapes or sheets. On the basis of the crystallographic and IR data, and the calculated energetics of hydrogen bonding, no significant differences are observed for tape vs sheet motifs. The rodlike arenedicarboxamides **1**−**4** adopt tape structures in which the hydrogen-bonded scaffold provides a 5 Å separation between the long axes of adjacent arenes. This scaffold permits individual arenes to adopt conformations similar to those observed in the vapor or solution phase. It also permits edge-to-face or herringbone interactions between adjacent arenes. The arenedicarboxamides **5** and **6** adopt sheet structures and have same calculated density. Their wider naphthalene shapes may prevent them from forming tapes with stabilizing arene−arene interactions or close packing between tapes. The highly puckered motif-B single-layer structure of **5** may be stabilized by close packing between sheets. Both intersheet face-to-face arene−arene interactions and C−H···O═C hydrogen bonding may contribute to the stability of the uncommon motif-C bilayer structure of **6.** Such weak interactions have an important role in determining the crystal-packing motif and molecular conformation of molecules whose partial crystal structure has been preorganized by hydrogen bonding.[28]

**Acknowledgment.** Financial support for this research has been provided by the National Science Foundation. We thank K. Poeppelmeier for the use of the differential scanning calorimeter and a reviewer for helpful suggestions.

**Supporting Information Available:** ORTEP drawings of the molecular structures and tables of positional and thermal parameters, bond lengths, and bond angles for **1**, **5**, and **6** (8 pages). See any current masthead page for ordering and Internet access instructions.

JA962986B